MOLECULARLY IMPRINTED MICROPARTICLES BASED ON QUATERNARY AMMONIUM SALTS FOR LIPOPOLYSACCHARIDE RECOGNITION

Ana-Lorena NEAGU[1], Ana-Mihaela GAVRILĂ[2], Bianca-Elena STOICA[3], Horia IOVU[4*], Cătălin ZAHARIA[5], Tanța-Verona IORDACHE[6*]

This work depicts the preparation of molecularly imprinted polymers (MIPs) via sol-gel method, further tested against lipopolysaccharide (LPS) from Gram negative bacteria. For this purpose, two types of microparticles of MIPs and NIPs (non-imprinted polymers, as control) were developed using quaternary ammonium salts (QAS) as stabilizers, namely vinyl benzyl trimethyl ammonium chloride (VBTAC) and sodium dodecyl sulphate (SDS). The presence of LPS inside the polymers was confirmed via FTIR and their microstructure was characterized by morpho-dimensional, thermogravimetric and nitrogen adsorption/desorption experiments. Adsorption studies evidenced the presence of binding cavities inside the VBTAC-based MIPs, proving that these particles were more efficient for LPS recognition, compared to the control NIP.

Keywords: molecularly imprinted microparticles, sol-gel, quaternary ammonium salts, LPS

1. Introduction

The spreading of multi drug resistant Gram-negative bacteria (GNB) has become a major cause of morbidity and mortality worldwide over the last decades due to its continuous mutations. These kinds of pathogens also known as 'superbugs' bacteria are widespread in the environment; *Pseudomonas aeruginosa* being one of the most frequently identified [1]. In healthcare systems, according to

[1] Scientific Researcher, PhD student Chim, National Institute for Research & Development in Chemistry and Petrochemistry ICECHIM, Romania, e-mail: ana-lorena.ciurlica@icechim.ro
[2] Scientific Researcher 2nd degree, PhD Eng, National Institute for Research & Development in Chemistry and Petrochemistry ICECHIM, Romania, e-mail: ana.gavrila@icechim.ro
[3] Scientific Researcher, PhD Eng., National Institute for Research & Development in Chemistry and Petrochemistry ICECHIM, Romania, e-mail: bianca-elena.stoica@icechim.ro
[4] Prof., Advanced Polymer Materials Group, University POLITEHNICA of Bucharest, Romania, email: horia.iovu@upb.ro
[5] Prof., Advanced Polymer Materials Group, University POLITEHNICA of Bucharest, Romania, email: zaharia.catalin@gmail.com
[6] Scientific Researcher 1st degree, PhD Eng., National Institute for Research & Development in Chemistry and Petrochemistry ICECHIM, Romania, *corresponding author, e-mail: iordachev.icechim@gmail.com

Centers for Disease Control and Prevention (CDC), *P. aeruginosa* is the most common disease-maker especially in patients with compromised immune systems with a number of 2700 estimated deaths in 2017 [2]. Regarding this aspect, in the same year, World Health Organization (WHO) released its first ever list of antibiotic-resistant "priority pathogens", where *P. aeruginosa* was classified with critical priority [3]. This list was considered a triggered alarm to urgent the public health needs and to encourage the researchers to enhance the development of new antibiotics and efficient low cost and simple methods to detect these bacteria in healthcare and environment. In recent years, the development of new materials capable of detecting toxic lipopolysaccharides (LPS, which compose the outer membrane of GNB) gained a lot of interest. Given that most of the procedures are quite accurate [4], the sample preparation processes instead, including costs and ruggedness, are difficult.

One strategy to accomplish fast, cost-effective, and efficient recognition for LPS is the molecular imprinting technology (MIT). The seemingly simple technique of MIT can be defined as a template-guided synthesis in self-assembly mode that leads to a molecular host [5]. MIT usually involves the polymerization and crosslinking of functional monomers in the presence of a template molecule, which interacts with the polymer network via specific interactions. After the removal of the template, specific binding cavities toward the target molecules are left in the resulting polymers. The complementary molecular information of the template is transposed into the polymer, endowing the final material with specificity and selectivity. Recently, our group used the combination between MIT and sol–gel techniques to prepare molecularly imprinted polymers (MIPs) able to recognize various hazardous molecules [6,7].

Because of its high molecular weight and amphiphilic (lipophilic and hydrophilic) nature, the molecular imprinting of LPS as template molecule is one of the most difficult topics in this research field [8]. Long *et al.* manufactured surface molecularly imprinted nanoparticles for targeting *P. aeruginosa* strains using an inverse microemulsion polymerization process. The resultant nanoparticles displayed preferential identification of *P. aeruginosa* by flow cytometry, as well as targeting *in vivo* in rabbit keratitis and mouse meningitis models [9]. Ma *et al.* developed molecularly imprinted polymers via photoinitiated bulk polymerization in order to reduce the bacterial biofilm formation of *P. aeruginosa* by capturing the 3-oxo-C12-AHL (used as template) who induces the quorum sensing at bacterial level. The final MIPs based on itaconic acid (IA) and 2-hydrox-yethyl methacrylate (HEMA) appeared to reduce almost 65% of the biofilm due to high adsorption affinity toward the template [10]. Stoica *et al.* recent paper described the behavior of screen-printed carbon electrodes (SPCE) modified with LPS-MIPs films able to recognize the bacterial endotoxins derived from *P.*

aeruginosa. The MIP films were obtained using a sol-gel mixture doped with zinc oxide and further deposited onto the working surface of a SPCE [11].

In this present work, the preparation of MIP particles with recognition cavities for lipopolysaccharides (LPS, the endotoxin component of GNB outer membrane) is also presented but using a sol-gel derived technique to obtain microparticles. The influence of the stabilizer upon the specificity of MIPs for recognizing LPS was evaluated using two quaternary ammonium salts (QAS) namely vinyl benzyl trimethyl ammonium chloride (VBTAC) and sodium dodecyl sulphate (SDS) as surfactants. QAS with 10–12 carbon chains typically have the strongest biocide activity but increasing the length of the alkyl chain can reduce the antimicrobial action [12]. On the other hand [13], QAS with vinyl group are among the most efficient and proper when are used as stabilizers or as functional monomers, which could enable synthesizing selective imprinted polymers for negatively charged target molecules as LPS [14].

Thereby, this paper reports the synthesis and characterization of organosilica LPS-MIPs based on tetraethyl orthosilicate (TEOS) as structural monomer and (3-aminopropyl) triethoxysilane (APTES) as co-monomer. The prepared MIPs particles were characterized by Fourier-Transform Infrared spectroscopy (FTIR), Scanning Electron Microscopy (SEM), Thermogravimetric analysis (TGA) and porosimetry measurements. The particles were further tested in terms of batch rebinding studies in liquid state *via* spectrophotometric techniques, to assess the effect of the stabilizer upon the specificity of prepared polymers.

2. Materials and methods

2.1. Materials

In order to obtain the sol-gel particles, the following monomers were used as received: tetraethyl orthosilicate (TEOS, 98%, Fluka, Fluka Chemie GmbH, Buchs, Switzerland) and (3-aminopropyl) triethoxysilane (APTES, 99%, Acros Organics, Pittsburgh, PA, USA). Sodium dodecyl sulfate (SDS, 95%) was purchased from Scharlab (Barcelona, Spain) and vinyl benzyl trimethylammonium chloride (VBTAC, 99%) was provided from Sigma Aldrich (St. Louis, MO, USA). Ethanol (EtOH, 99.5%) and ammonium hydroxide (NH_4OH, 25%) were supplied from ChimReactiv (Ion Creanga, NT, RO). The template lipopolysaccharide from *Pseudomonas Aeruginosa* 10 (LPS, 500,000 E.U/mg, Sigma-Aldrich, St. Louis, MO, USA) was used as a lyophilized powder without further purification. Distilled water was used to prepare all the samples.

2.2. Synthesis of LPS-MIPs microparticles

Two series of imprinted microparticles (i.e., MIP SDS and MIP VBTAC) were synthesized *via* sol-gel, where TEOS was used as structural monomer, APTES as functional monomer and VBTAC or SDS as stabilizers [15]. Briefly, a typical

MIP batch consisted in mixing two solutions (referred to as Sol A and Sol B) at room temperature (25 °C), which contained the precursor gel solution and the catalytic medium respectively, as presented in **Fig. 1**. The precursor solution was prepared by the dissolution of TEOS (24 mmol), together with APTES, (24 mmol), VBTAC or SDS (4,7 mmol) and LPS (0,000232 mmol) in ethanol (81 ml). The catalytic medium contained of an aqueous solution of 25% ammonium hydroxide (1:3 NH_4OH/ H_2O molar ratio). After 10 minutes of purging with nitrogen gas, the precursor gel solution was gradually added to the catalytic medium in droplets and mechanically stirred at 200 rpm for 2 h. During the reaction, the partial hydrolysis of -OH groups and aldol polycondensation takes place. The formed microparticles were separated from the reaction medium by centrifugation (7500 rpm) and washed two times with distilled water to remove unreacted monomers, surfactant. In order to extract the template, LPS, the microparticles were washed two times with 0.1 N sodium hydroxide solution, followed by another washing cycle with distilled water. Each washing cycle was realized by centrifugation at 7500 rpm for 30 min. The polymers were further dried at room temperature (25 °C) for 48 hours and then in a vacuum oven (at 60 °C) for other 48 hours. The same synthesis procedure was used to obtain the non-imprinted control particles (noted by analogy NIP SDS and NIP VBTAC) but without adding the LPS template.

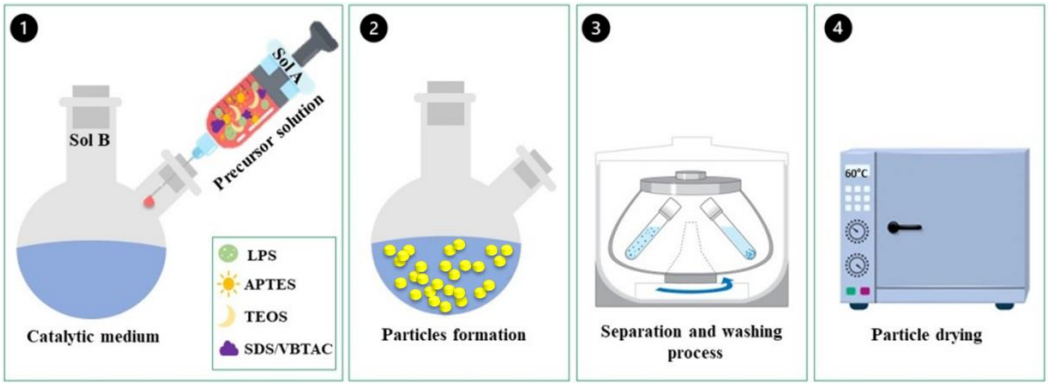

Fig. 1. Synthesis steps of LPS-MIPs microparticles

2.3 Characterization methods

The structure of the obtained MIPs and NIPs particles was analyzed using Nicolet Summit Pro FTIR device equipped with an ATR-diamond accessory (Thermo SCIENTIFIC) in the range 4000-500 cm^{-1}. The morphology of microparticles was highlighted using Scanning Electron Microscopy Quanta Inspect F (Waltham, MA) equipped with a field emission gun (FEG) with 1,2 resolution and an energy-dispersive X-Ray spectrophotometer. The particle sizes of control and imprinted particles were determined by dynamic light scattering (DLS) analysis using a Malvern Zetasizer Nano-ZS (Malvern Instruments,

Worchestershire, UK) system equipped with a 4 mW He–Ne laser (633 nm). Thermal stability of polymers was investigated using a Thermogravimetric STA 449C Jupiter analyzer coupled with an Aeolos II MS (STA-MS, 2007, Netzsch Gmbh, Germany) detector, under helium atmosphere at a 5 °C/min heating rate. Prior to adsorption-desorption measurements in nitrogen, samples were degassed at 373.15 K for 3 h under vacuum (p <102 Pa) to eliminate adsorbed gas and moisture. Surface areas and pore volumes were determined on a volumetric adsorption analyzer Quantachrome Nova2200e (Quantachrome Instruments USA), at the liquid nitrogen temperature. The LPS batch re-binding experiments were performed using a Thermo Scientific™ Evolution™ UV-Vis 260 BIO spectrophotometer (Walthman, MA, USA) in the 200-500 nm wavelength region, with 10 mm quartz cuvettes.

2.4. Batch Binding Measurements on microparticles

Batch binding assays were performed to evaluate the LPS adsorption performance of MIPs and NIPs particles. The calibration of LPS at λ_{max} = 256 nm was obtained in water using a series of standard solutions containing LPS in the endotoxin units (EU/L) range i.e., 250-90 EU/L concentration. 30 mg of MIPs or NIPs particles were contacted with 3 mL LPS solution of 154 EU/L concentration (experiments conducted in duplicate) and stirred for 15 min at 25 °C. Supernatants were collected after 6 h and 24 h, in order to evaluate the remaining LPS in solution by UV-Vis. The adsorption capacity of MIPs and NIPs (Q) for LPS was calculated according to equation (1), where $C_{N,i}$ (E.U/L) and $C_{N,f}$ (E.U /L) were the LPS initial and final concentration, respectively, in the feed solution; V_s(L) is the volume of the initial feed solution; m_p (mg) is the weight of polymeric particles.

$$Q = \frac{(c_{N,i} - c_{N,f}) \cdot V_s}{m_p} \tag{1}$$

The imprinting factors calculated according to equation (2) (where: Q_{MIP} and Q_{NIP} were the re-binding capacities of MIP and NIP (E.U/g), respectively), quantified the specificity with which MIP particles re-bind LPS, versus the NIP.

$$F = \frac{Q_{MIP}}{Q_{NIP}} \tag{2}$$

3. Results and discussion

3.1 Structure and composition of MIP and NIP microparticles

FTIR spectroscopy was employed for underlining the structure of the polymers and, more specifically, the imprinting effect and the conditioning procedure, for the MIPs after template removal (noted MIP extracted). Comparing

all FTIR spectra (Fig. 2), the obtained polymer particles present some similarities, keeping the same pattern in terms of characteristic bands provided by the organic-inorganic matrix. The bands assigned to the stretching vibrations ν_{-CH2} and ν_{-CH}, in aminopropyl and ethoxy groups, characteristic to the organic fragments of the monomer APTES, can be observed in all spectra (Fig. 2a and b) between 2930-2945 cm^{-1}. The regions between 1100–900 cm^{-1} and 550-400 cm^{-1} are representative for the characteristic bands of the (SiO) backbone network. For instance, the presence of the $-NH_2$ end group (deformation vibration δ_{-NH2}) from APTES is underlined through the overlap with the band recorded at 1638 cm^{-1}.

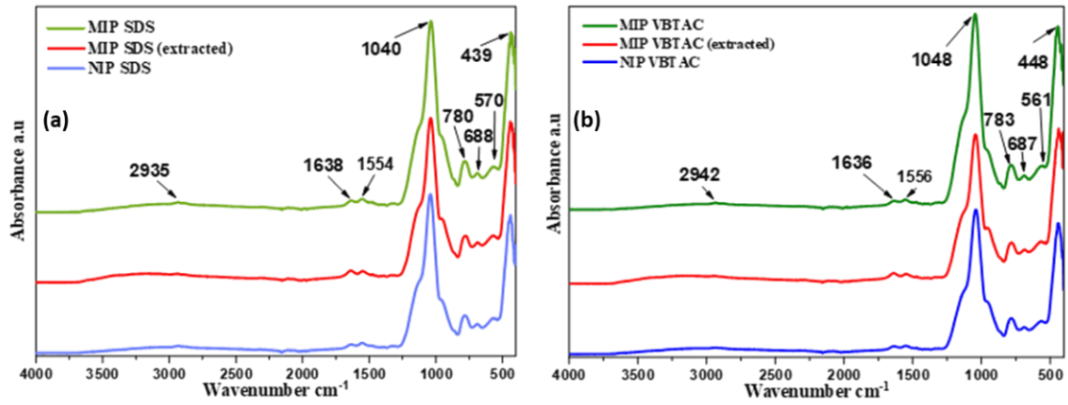

Fig. 2. FTIR spectra of (a) MIP SDS and (b) MIP VTAC, before and after LPS removal (MIP SDS extracted and MIP VBTAC extracted) compared to those of NIP SDS and NIP VBTAC

The effect of molecular imprinting with LPS is underlined by the intensity of the bands recorded around 1638 and 1554 cm^{-1} attributed to I and II amide characteristic to Lipid A (in LPS). Another hint to LPS imprinting was given by the increased intensity of the band recorded at 1048 cm^{-1} in the spectrum of MIP VBTAC due to specific interactions of the -Si-O-Si- network with the template molecule. In this case, phosphoryl bands from LPS at 1048 cm^{-1} [16, 17]) overlap with the specific -Si-O-Si- bands from the polymer [18]. It can also be noted that the distinctive LPS bands, in the region between 1630-1560 cm^{-1} and 1040 cm^{-1}, are attenuated in the spectra of extracted MIPs (the spectra resembling more to those of the corresponding NIPs). This observation points out toward a successful extraction of LPS, in which case it can be assumed that specific cavities for LPS recognition may have formed. Traces of the stabilizer (ν_{-N-CH3} and δ_{-N-CH3}) were detected in all spectra at 950 and 1339 cm^{-1}, respectively. The band recorded at 690 cm^{-1}, can be correlated with the deformation of the $-CH_2Cl$ group within VBTAC stabilizer [19].

3.2 Particle size and morphology of MIP and NIP microparticles

For both series, the non-imprinted particles (NIPs) presented aggregates and bimodal size distributions. According to Fig. 3c and d, the main peak corresponded to particles with an average hydrodynamic diameter between 425 and 590 nm, while the second peak to 85-141 nm sized particles. This secondary peak can be associated to independent nanoparticles, which associate dynamically to generate micro-aggregates. Therefore, in the case of NIPs, controlling the mean particle size by surfactant addition has somehow failed. Nevertheless, the same surfactants in MIPs formulation have successfully delivered monomodal microparticles with a narrower size distribution (Fig. 3a and b). This can be explained by the co-surfactant effect of the LPS template, which is an amphiphilic large molecule. As a result, another conclusion can be drawn from this observation, that imprinting of LPS was epitope (involving only the lipid fragment called Lipid A) and occurred at the surface of particles.

SEM micrographs of MIPs and NIPs (Figs. 4 and 5) revealed relatively porous and quite regular spherical micro/nanoparticles in various aggregates. Comparing the NIPs with the MIPs, some morphology differences in particle shape and size occurred due to stabilizers. NIPs particles presented more porous surfaces compared to the MIPs, leading to a more pronounced coalescence phenomenon (as confirmed by DLS). MIPs exhibited a compact and homogenous morphology, with bigger pore diameters, due to the self-assembly between the monomers and the template molecule [11]. The use of SDS as stabilizer led to some irregular and robust particles but relatively smooth in the similar size range (85-530 nm) (Figs. 4 a and b). These results suggest that SDS was not able to reduce the increased interfacial tension of the particles causing the coalescence of the particles in cluster aggregates by mutual collision [21, 22]. For microparticles with VBTAC as stabilizer, more defined particles with diameters varying from 141 to 590 nm were obtained (Figs. 5 a and b).

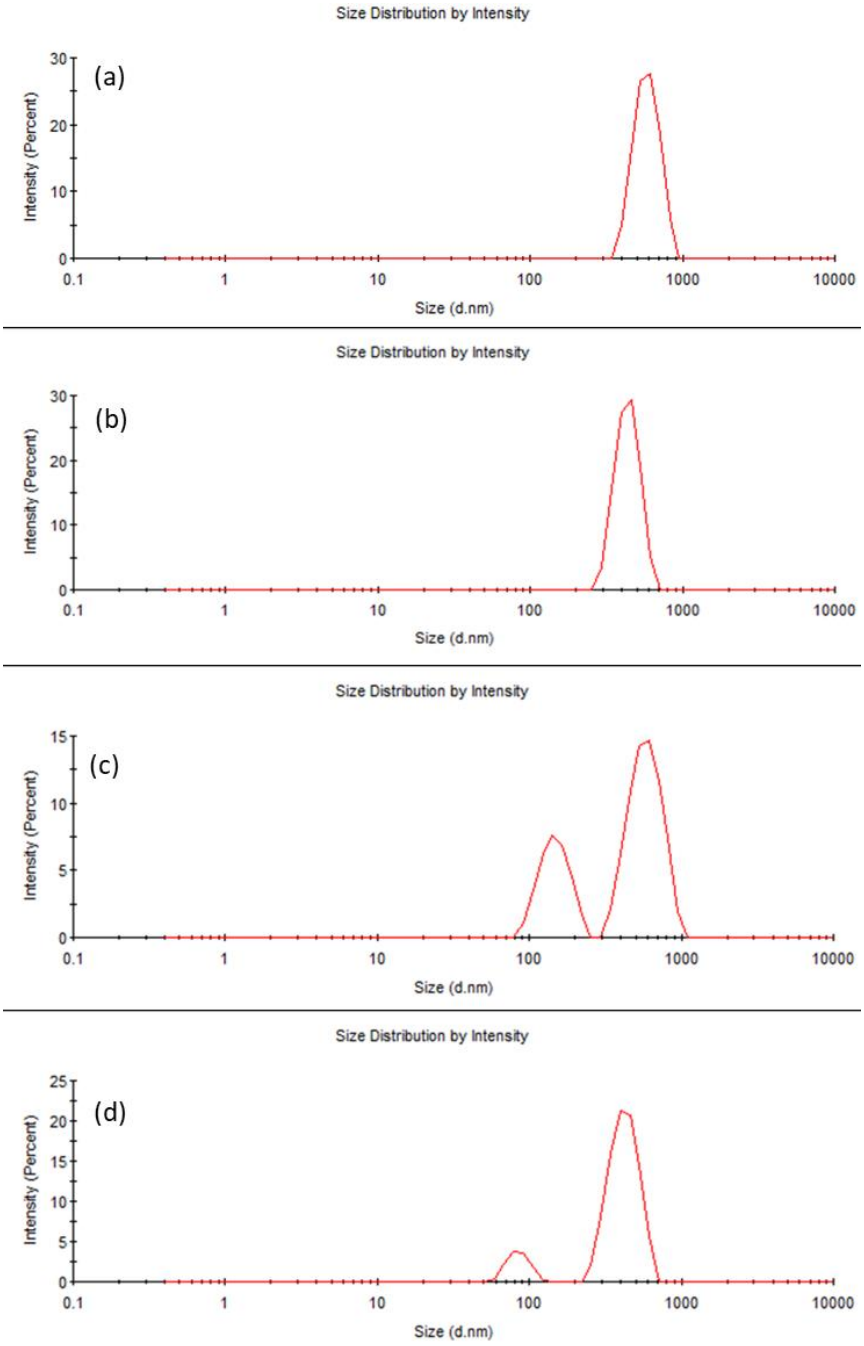

Fig. 3. Dimensional distribution by dynamic light scattering of a) MIP VBTAC, b) MIP SDS, c) NIP VBTAC and d) NIP SDS particles

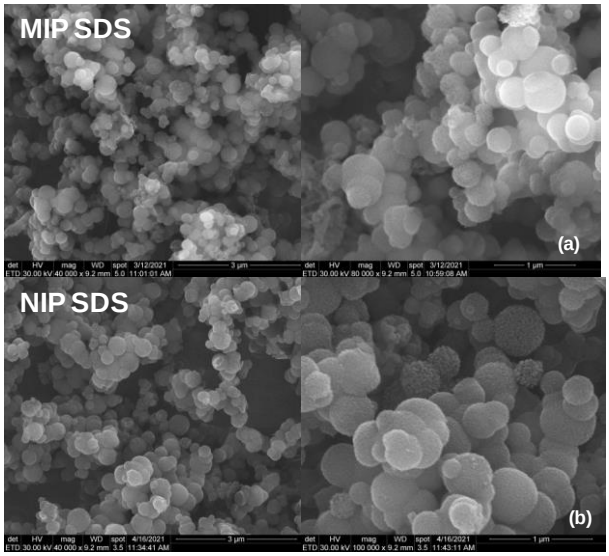

Fig. 4. SEM micrographs of (a) MIP SDS and b) NIP SDS at two different scales 3 μm and 1 μm

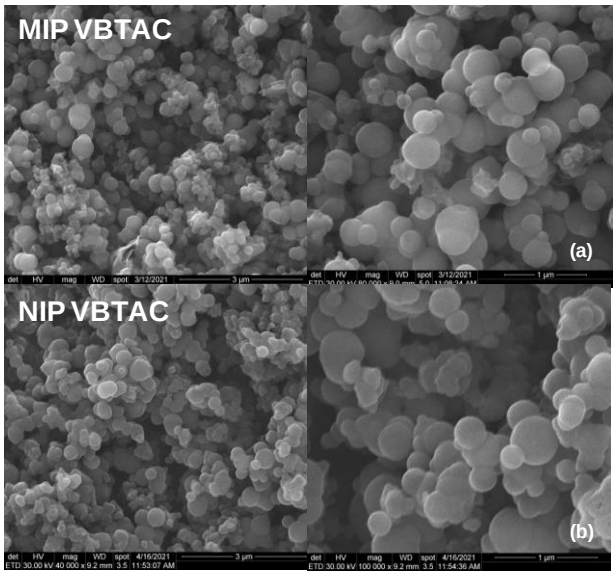

Fig. 5. SEM micrographs of (a) MIP VBTAC and b) NIP VBTAC at two different scales 3 μm and 1 μm

3.3 Porosimetry measurements of MIP and NIP microparticles

The N_2 absorption-desorption isotherms (Fig. 6) using the BET method allowed the measurement of BET specific surfaces area, pores volume (Vp), pore specific surface area (S_{BET}) and pore average diameter (Dp) of the LPS-MIPs and their corresponding control NIP particles (values presented in Table 1).

Pore size distribution, analysed according to the Barrett-Joyner-Halenda model (BJH), indicates a majority of mesopores and a small number of micropores (Fig. 6, insets). The pore size distribution was obtained from the desorption data. MIPs particles registered two representative peaks that suggest the majority presence of mesopores with diameters between 2.8 and 7 nm, while in the case of NIPs, two representative peaks for mesopores at 2.5 and 7 nm diameter were observed. For MIPs extracted, four representative peaks between 2.5 and 13 nm were recorded. The wider pore diameter range of these particles suggests the appearance of specific binding cavities, proving that specific cavities for LPS were successfully created after extraction. The porosimetry values referred to an average pore diameter between approximately 1.54 and 2.90 nm, a specific BET surface area from 9.93 to 24.62 m^2/g, a pore surface area between 8.13 and 18.99 m^2/g, as well as a total pore volume between 0.02 and 0.05 cm^3/g, which demonstrate textural similarities between MIPs and NIPs particles (Table 1).

Table 1

Nitrogen adsorption-desorption obtained values for MIPs, MIPs extracted and NIPs.

Sample	BET Specific surface (S_{BET}, $m^2\ g^{-1}$)	Pore surface area (BJH) (Ap, $m^2\ g^{-1}$)	Pore diameter from desorption (BJH) (Dp, nm)	Pore volume (BJH) (Measured at P/P0 = 0.99) (Vp, $cm^3\ g^{-1}$)
MIP SDS	9.93	8.13	2.90	0.02
MIP SDS extracted	20.92	15.13	2.90	0.04
NIP SDS	12.57	8.59	2.78	0.02
MIP VBTAC	13.97	9.74	2.90	0.02
MIP VBTAC extracted	24.62	18.99	2.90	0.05
NIP VBTAC	17.71	13.03	1.54	0.03

These results are mainly due to the organosilane monomer (APTES) and the porogenic solvent [19, 23], in this case ethanol. The formation of specific cavities can be particularly associated with the higher specific surface areas formed after LPS extraction, i.e., MIPs extracted. The pore surface area as well as the pore volume also increase due to LPS cleavage from the matrix. These values also indicate that no pore collapse was registered during LPS extraction due to the very stable polymer network.

In the case of MIPs extracted (Fig. 6c-d), wider hysteresis was observed compared to the MIPs (at relative pressure P/P_0 between 0.5 and 1) as well as a total N_2 desorption. The adsorption-desorption isotherms of all polymer particles were characteristic to type II with a type IV allure suggesting the formation of mesopores. MIPs and NIPs particles show H3 type hysteresis curve where capillary condensation takes place at lower relative pressure ($P/P_0 > 0.3$), noting that the adsorbed gas is not completely desorbed (crossover between adsorption and desorption curve). at $P/P_0 = 0.3$.

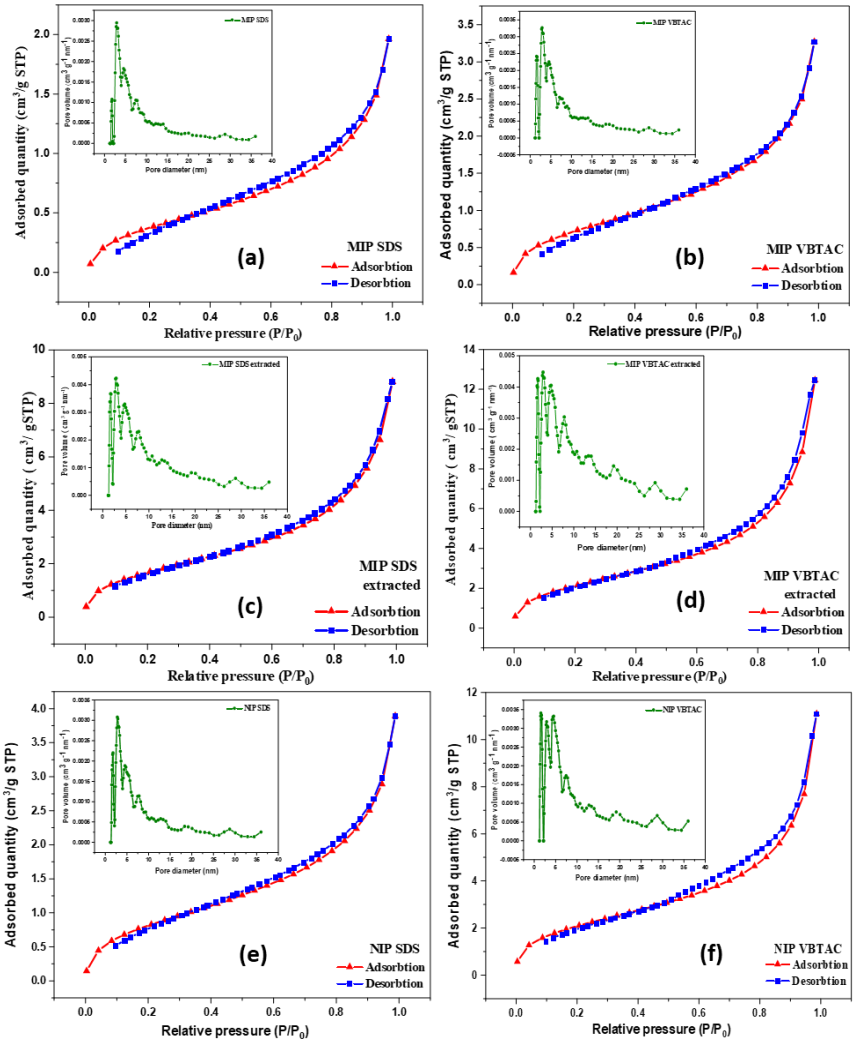

Fig. 6. Nitrogen adsorption/desorption isotherms at 77 K for (a) MIP SDS, (b) MIP VBTAC, (c) MIP SDS extracted, (d) MIP VBTAC extracted, (e) NIP SDS, (f) NIP VBTAC and particles size distribution (inset figures)

3.4 Thermal analysis of MIPs and NIPs microparticles

The thermal degradations of imprinted MIP VBTAC and MIP SDS and their non-imprinted counterparts indicate quite similar behaviour. All particles show a first stage of mass loss in the temperature range 30–100°C, which can be attributed to the elimination of moisture (Fig. 7a). In the temperature range of 120-400 °C, fragments such as formyl, acetyl or amine are detached from the organosilane structure and between 400 and 700 °C the organic fragments methyl, ethyl are completely decomposed resulting a residual mass of 71-78 % [19]. Since the MIPs

were analysed before LPS extraction, a higher mass loss was observed compared to their NIP counterparts and may be attributed to the decomposition of LPS. Another interesting remarque about MIP decomposition is the appearance of a shoulder around 650 °C (Fig. 7b), for both series (MIP VBTAC and MIP SDS). According to the European Pharmacopoeia [20] there are two depyrogenation time-temperature combinations which can be used for LPS, eg. 200°C for 60 min or 250°C for at least 30 min with the mention that an increased temperature will shorter the degradation time. Therefore, based on this aspect, a clear difference in the structure of the MIPs have occurred due to LPS imprinting. It can be assumed that the interactions between TEOS/APTES and template molecule can affect the initial nature of the mesophase (i.e., micelle's composition).

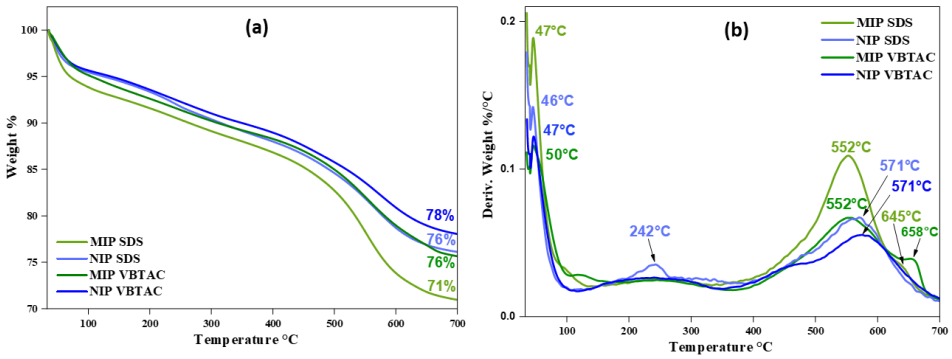

Fig. 7. TGA (a) and DTG (b) curves of the obtained MIPs and NIPs particles.

3.5 Rebinding experiments of LPS on MIPs and NIPs

Adsorption parameters of MIPs and NIPs are shown in Table 2. It can be observed that both systems present very low specificity in the first 6 h, after which the MIP exhibits a more pronounced adsorption of LPS. Although the adsorption capacity for LPS was lower compared to that registered for MIP SDS, it seemed that only MIP VBTAC was able to retain specifically LPS after 24 h (imprinting factor of 1.79). The difference between the two MIPs binding affinity clearly indicated the role of the surfactant in the imprinting process with major impact on the formation of specific binding sites. Thereby, in the case of MIP SDS the surfactant addition was not very effective towards binding cavity formation, possibly due to SDS adsorption to the hydrophobic regions of LPS [24]. Rebinding of LPS on the obtained MIPs and NIPs particles compared to other reported values of imprinting factor (for instance, 1.68 for MIPs-based on itaconic acid, [10]), indicated that important advancements in the preparation of performant MIPs for LPS recognition may be brought using sol-gel techniques and small molecule surfactants, such as VBTAC.

Table 2

The obtained adsorption capacities and imprinting factors at 6h and 24h respectively for the polymeric systems MIP/NIP VBTAC; MIP/ NIP SDS.

Sample	Q_{MIP} (E.U/g)		Q_{NIP} (E.U/g)		F	
Time (h)	**6**	**24**	**6**	**24**	**6**	**24**
MIP/NIP SDS	2.48	6.59	4.07	8.14	0.61	0.81
MIP/NIP VBTAC	6.94	4.45	7.59	2.47	**0.91**	**1.79**

4. Conclusions

Molecularly imprinted polymer microparticles able to recognize and rebind LPS from *Pseudomonas Aeruginosa,* and their blank correspondents, were successfully synthesized *via* sol-gel derived technique, using VBTAC and SDS as surfactants. The resulted MIP and NIP microparticles were characterized using morpho-structural, thermogravimetric and porosimetric methods, in which case important differences were observed between the two series, underlining a rather synergic effect of LPS and VBTAC upon the morphology, the particle size and uniformity, and the thermal decomposition behaviour. Furthermore, the MIPs and NIPs microparticles were tested for LPS rebinding from synthetic solutions, at different contact times, and revealed that the MIP VBTAC microparticles were able to rebind LPS, in smaller amounts compared to MIP SDS, but with a two-fold greater specificity (imprinting factor of 1.79 after 24h). Therefore, using a small molecule surfactant, such as VBTAC, to prepare LPS-MIP microparticles by sol-gel, seems to be a step forward in achieving higher efficiency for recognizing LPS from *Pseudomonas Aeruginosa*.

Acknowledgements

The authors thank for financially support the Romanian Funding Agency UEFISCDI the Ministry of Research, Innovation and Digitalization for funding the projects (255PED/2020 TOXINSENS) and the Ministry of Investments and European Projects through the Human Capital Sectoral Operational Program 2014-2020, Contract no. 62461/03.06.2022, SMIS code 153735.

R E F E R E N C E S

[1] *B. Sharma et al*, "Superbugs: The Nightmare Bacteria", Journal of Animal Research, **vol.11**, no.5, Oct 2021, pp. 765-773.

[2] *CDC*. "Antibiotic Resistance Threats in the United States2019", Atlanta,GA: U.S. Department of Health and Human Services CDC, 2019, pp. 97-98.

[3] *E. Tacconelli et al*, "Global priority list of antibiotic-resistant bacteria to guide research, discovery, and development of new antibiotics", World Health Organization, Feb 2017, 1-7.

[4] *L. Varadi et al*, "Methods for the detection and identification of pathogenic bacteria: past, present, and future", Chemical Society Reviews, **vol. 46**, no. 16, Aug 2017, pp. 4818-4832.

[5] *S. Piletsky et al, "*Molecularly Imprinted Polymers forCell Recognition", Trends in Biotechnology, **vol. 38**, no. 4, 2020, pp. 368-387.
[6] *A-M.Gavrila et al*, "Molecularly imprinted films and quaternary ammonium-functionalized microparticles working in tandem against pathogenic bacteria in wastewaters", Journal of Hazardous Materials, **vol.399**, 2020, 123026, pp. 1-12.
[7] *A-M.Gavrila et al*, "Role of Functional Monomers upon the Properties of Bisphenol A Molecularly Imprinted Silica Films", Applied Science, **vol.11**, 2021, 2956, pp. 1-16.
[8] *K-I. Ogawa et al*, "Development of lipid A-imprinted polymer hydrogels that selectively recognize lipopolysaccharides", Biosensors and Bioelectronics, **vol. 38**, June 2012, pp. 215-219.
[9] *Y. Long et al*, "Novel polymeric nanoparticles targeting the lipopolysaccharides of Pseudomonas aeruginosa" International Journal of Pharmaceutics, 502, Feb. 2016, pp. 232–241.
[10] *L. Ma et al, "*Development of Molecularly Imprinted Polymers To Block QuorumSensing and Inhibit Bacterial Biofilm Formation", ACS Applied.Material. Interfaces **vol.10**, 2018, pp. 18450−18457.
[11] *B. E. Stoica et al*, "Uncovering the behavior of screen-printed carbon electrodes modified with polymers molecularly imprinted with lipopolysaccharide", Electrochemistry Communications, **vol. 124**, Feb. 2021, 106965.
[12] *A-M. Gavrila et al*, "Synthesis and properties of organosilica particles with quaternary ammonium bearings as bacteriostatic interfaces", U.P.B. Sci. Bull., Series B, **vol. 83**, Iss. 3, 2021, pp. 215-230.
[13] *M. Zarejousheghani et al*, "Rational Design of Molecularly Imprinted Polymers Using Quaternary Ammonium Cations for Glyphosate Detection", Sensors, **vol. 21**, no. 296, Jan. 2021, pp. 1-18.
[14] *Y.Rosenfeld, Y.Shai,* "Lipopolysaccharide (Endotoxin)-host defense antibacterial peptides interactions: Role in bacterial resistance and prevention of sepsis" Biochimica et Biophysica Acta no. 1758, May 2006, pp. 1513–1522.
[15] *C. Yague, M. Moros, V. Grazu, M. Arruebo and J. Santamaria*, in J. Chem. Eng., **vol. 137**, 2008, pp. 45-53.
[16] *E. C. Yi and M. Hackett*, "Rapid isolation method for lipopolysaccharide and lipid A from Gram-negative bacteria", Analyst,**vol. 125**, Mar. 2000, pp. 651–656.
[17] *A. Barkleit et al*, "Coordination of uranium (VI) with functional groups of bacterial lipopolysaccharides studied by EXAFS and FT-IR spectroscopy", Dalton Trans., **vol. 40**, July 2011, pp. 9868-9876.
[18] *M. E. Mathew et al*, "Synthesis and characterization of poly (benzyl trimethyl ammonium chloride) ionic polymer", AIP Conference Proceedings, **vol. 1940**, 2018, pp.1-6.
[19] S. *J. Parikh, J.Chorover*, "ATR-FTIR study of lipopolysaccharides at mineral surfaces", Colloids and Surfaces B: Biointerfaces, **vol.62,** Oct 2007, pp. 188-198.
[20] *Council of Europe*, "European Pharmacopoeia", 8th ed.; Council of Europe: Strasbourg, France, 2007; **vol. 2**, pp. 1949–1951. ISBN 978-92-871-7525-0.
[21] *E. Cáceres et al*,"Preparation of molecularly imprinted polymers for diphenylamine removal from organic gunshot residues", Journal of the Chilean Chemical Society, **vol. 59**, no. 4, 2014, pp. 2731-2736.
[22] *Z-B. Zhang et al*, "Micronization of silybin by the emulsion solvent diffusion method",*International Journal of Pharmaceutics*, **vol. 376**, May 2009, pp. 116-122.
[23] *V.N. Goral, N. Zaytseva,A.J Baeumner*. "Electrochemical microfluidic biosensor for the detection of nucleic acid sequences", Lab Chip, **vol. 6**, Jan 2006, pp. 414-421.
[24] *N. Inoue, T. Ooya, T. Toshifumi*, "Hydrophilic molecularly imprinted polymersfor bisphenol A prepared in aqueous solution", Microchim Acta, **vol. 180**, 2013, pp. 1387–1392.